Estimation of Water Depth of Shallow Rivers by Analyzing Optical Remote Sensing Images Captured with a Drone

Byoung Gil Choi,[1] Yong Hee Kwon,[1] Jun Hee Lee,[1] and Young Woo Na[2*]

[1]Department of Civil and Environmental Engineering, Incheon National University,
119, Academy-ro, Yeonsu-gu, Incheon 22012, Republic of Korea
[2]Department of Civil Engineering, Semyung University,
65, Semyeong-ro, Jecheon-si, Chungcheongbuk-do 27136, Republic of Korea

In this study, we developed a method for estimating the water depth of shallow rivers by analyzing images captured with a drone, using optical remote sensing techniques. In an attempt to compensate for the shortcomings of existing surveying methods, optical-remote-sensing-based methods are being actively developed, but environmental conditions and data processing methods for application to rivers have not yet been sufficiently optimized. Here, we present an equation for estimating the water depth of shallow rivers from drone images and field survey results acquired under various conditions, and we aimed to verify accuracy using checkpoints. We found that estimating the water depth by calculating the parameters using multiple linear regression analysis based on the pixel values of each band of the image and the field-surveyed water depth is more efficient than the conventional field survey method. In addition, the use of high-resolution images taken at noon without shadows and the removal of reflected light using a polarizing filter proved to be effective approaches in that nearly 88% of the images were within the acceptable range for bathymetry and about 94% were within the acceptable range when converted to low resolution. Finally, estimation of the water depth using the optical remote sensing technique indicated that the accuracy was low for deep water and that pixel values could be distorted by water plants or shadows.

1. Introduction

In this study, we aimed to develop a method for estimating the water depth of shallow rivers using optical remote sensing techniques to capture drone images for subsequent analysis. Conventional techniques for surveying rivers rely on direct survey methods that use the Global Navigation Satellite System (GNSS) and the total station. Existing indirect survey methods include the use of acoustic sounders or aerial light detection and ranging (LiDAR). Acoustic sounders can measure large areas of deep water in a short time, and aerial LiDAR can simultaneously measure the land and seabed terrain.[1]

However, direct measurement methods such as those based on GNSS are prone to accidents because it is necessary to enter the water directly and measurements with uniform accuracy are not possible. The disadvantage of using an acoustic sounder is that the sensor must be immersed in water and mounted on a ship, which makes it difficult to conduct measurements in shallow water with depths of 0.5 m or less. Although LiDAR can be used to measure shallow water areas, it has the disadvantage of excessive cost. Current research aims to overcome the shortcomings of existing bathymetry methods for measuring the depth of shallow water. A shallow stream is usually defined as a stream with a depth of 5 feet (approximately 1.5 m) or less. Ehses and Rooney suggested that the multispectral image of the WorldView-2 satellite is within the allowable depth of up to 20 m,[2] and Lee *et al.* applied aerial depth LiDAR data with the Adaptive Triangular Irregular Network ground filtering technique to achieve an accuracy of about 88.8% at a maximum depth of 2.2 m.[3] Oh *et al.* presented a method for capturing and analyzing drone images with a spatial resolution of 2.5 cm of shallow waters near the coastline with depths of up to 5 m using optical imaging techniques,[4] whereas Holman *et al.* examined the accuracy of topographic surveys using drones, and in particular, analyzed sea level images taken by drones to assess the accuracy of this method for measuring depth.[5] Yi *et al.* studied bathymetry in shallow waters using aerial photographs and presented results with error within 0.1 m for areas in which the water was no more than 10 m deep.[6] Yeo *et al.* suggested that it was possible to use a drone to survey a river with depth within 0.5 m for rivers with varying regional characteristics such as the flow rate, swell, and turbidity.[7] Choi and Na estimated the depth of a shallow river using a spatial resolution within 1.5 m and an image processing method to analyze images that were taken using a polarization filter.[1] However, they did not report the limits or conditions under which the depth can be estimated using photographs alone. This prompted our study, in which we determined the limits of the water depth and environmental conditions under which the depth of shallow river areas can be accurately measured using high-resolution drone images with a spatial resolution of 1 cm, which were captured using optical remote sensing techniques. In this study, as shown in Fig. 1, aerial photographs taken under various conditions, such as different spatial resolutions, with and without the removal of reflected light, and different shooting times, were analyzed. The GNSS coordinates of directly surveyed reference points were used to derive a formula for estimating the depth of a shallow river, and to verify the accuracy with the aid of checkpoints.
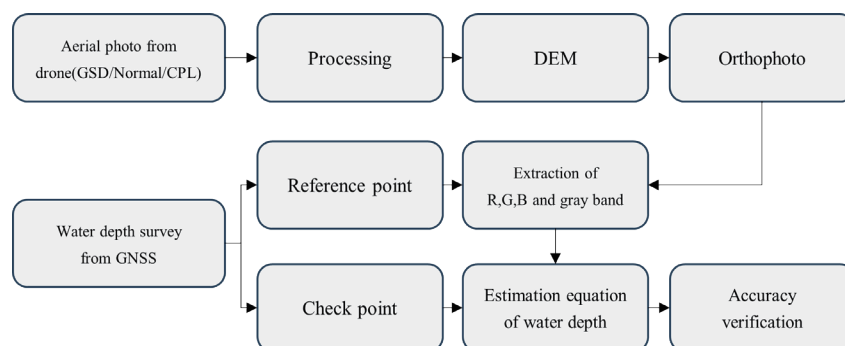

Fig. 1.   (Color online) Conceptual diagram of method for estimating the water depth of shallow rivers.

2.   Methods

2.1   Water depth estimation method using optical remote sensing technique

Optical remote sensing techniques for bathymetry include bathymetry models derived from the Beer–Lambert Law [Eq. (1)], which is based on the principle that the light that penetrates water is absorbed by the water, whereby the light intensity is weakened.[4]

$$I = I_0 e^{-\beta z} + I_w \tag{1}$$

Here, I is the intensity of light detected by the measuring device, I_w is the intensity of light reflected from the surface of the water, I_0 is the intensity of light transmitted through the surface and reflected from the bottom of the water, and β is the absorption coefficient (in clear water, the value depends on the frequency of the light).

Equation (1) can be rearranged such that it expresses the depth (z) as

$$z = \left\{ \ln\left(I_0\right) - \ln\left(I - I_w\right) \right\} / \beta. \tag{2}$$

An image captured by a drone consists of bands of visible light (red, green, and blue), and the digital number (DN) of the image has a value proportional to the light intensity. Because the values of the absorption coefficient in Eq. (2) differ depending on the color and turbidity of the water, atmospheric conditions, altitude of the sun, and so forth, Eq. (2) cannot be applied to the drone image as it is, and the intensity of the light reflected and transmitted from the surface of the water also changes.[4] In addition, Philpot proposed a method for quantifying the physical properties of water and estimating the situational depth in accordance with the characteristic changes in relation to Eq. (2).[8] However, his method was developed for multispectral satellite images captured at wavelengths other than those of visible light, such as near infrared and infrared, and it is difficult to apply when using only visible light bands as in our study. Accordingly, Lyzenga *et al.* presented a depth estimation formula using two spectral bands, as shown in Eq. (3), assuming that the physical properties of the bathymetry site are constant.[9]

$$Z = h_0 - \sum_{j=1}^{n} h_j \ln\left(band_j\right) \tag{3}$$

Equation (3) can be used to calculate the depth of some points in one image and determine each parameter through multiple linear regression analysis. However, considering that Eq. (3) is not fully compatible with ordinary cameras that use only visible light bands, the estimation would be more accurate with Eq. (4), which does not determine the natural logarithm.[2]

$$Z = a_0 - \sum_{j=1}^{n} a_j \left(band_j\right) \tag{4}$$

Yeo *et al*. proposed a method for depth estimation by combining each of the different bands using an artificial neural network and obtained the most accurate results for the combination of four bands: red, green, blue, and gray.[7] However, the disadvantage of analysis with the aid of artificial neural networks is that the physical properties cannot be determined.[4] Therefore, in this study, a depth estimation formula was derived by finding the parameters using the combination of the four bands of red, green, blue, and gray and the multiple linear regression analysis of Eq. (4). The gray band is usually calculated as $(R_{band} + G_{band} + B_{band})/3$, but in this calculation, the gray band can be calculated with Eq. (5) because it is the same as the result of using only the R, G, and B bands by linearity.[1]

$$Gray_{band} = \sqrt{(G_{band})^2 + (B_{band})^2 + (R_{band})^2} \tag{5}$$

Here, $Gray_{band}$ is the DN of the gray band, R_{band} is the DN of the red band, G_{band} is the DN of the green band, and B_{band} is the DN of the blue band.

By calculating the pixel value of the gray band using Eq. (5) and deriving the parameters for each pixel value through multiple regression analysis, the depth estimation formula can be derived as below.[1]

$$y = R_{band} \cdot x_1 + G_{band} \cdot x_2 + B_{band} \cdot x_3 + Gray_{band} \cdot x_4 + C \tag{6}$$

Here, *y* is the water depth, *x* is the parameter for the DN of each band, and *C* is a constant.

2.2 Method for removing reflected light from the surface using a polarizing filter

A polarizing filter is mainly used to remove reflected light from glossy objects such as the surfaces of glass or water. The surface of the water spreads the light reflected from the light source irregularly, and by using a polarizing filter, only the light traveling in a certain direction is transmitted and the remaining light is blocked to enhance the transparency of the image. In this study, the accuracy of the water depth estimation was assessed by comparing images without and with the removal of light reflected from the surface of the water using a circular polarizing filter (CPL: circular polarizing linear) for the DJI Mavic 2 Pro drone supplied by DJI Corporation.

3. Experiments and Analysis

3.1 Selection of target area for the study

In this study, as shown in Fig. 2, the study area was the upper reaches of the Nam River located in Hamyang County, Gyeongsangnam, where the average depth is 0.8 m and maximum depth is about 2.0 m, which can be directly measured by GNSS.
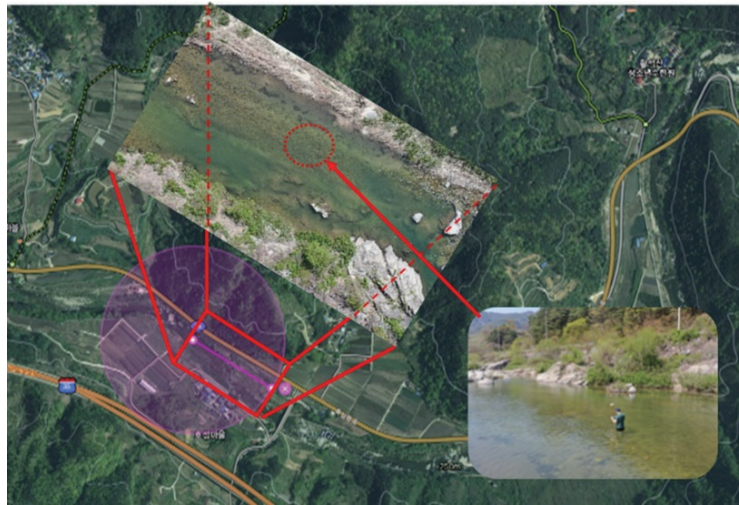
Fig. 2.   (Color online) Aerial view of the area selected for this study.

In addition, this part of the river has a gentle slope, the flow rate of the water is neither fast nor slow, and the water has acceptable turbidity such that the bottom of the river can be visually identified. Thus, this section of the river was selected as the target area for testing.

To optimize the conditions for depth estimation, photographs were captured at different times of the day (10:00, 12:00, and 15:00) to analyze the effect of shadows in accordance with the shooting time to determine whether a polarization filter should be applied to analyze the effect of the reflection of surface light. Spatial resolutions of 1 and 2.5 cm were used to analyze the effect of the spatial resolution. Fourteen sets of conditions (cases) were set (Table 1). The spatial resolutions of 5 and 10 cm were added by converting the ortho-image with the most accurate conditions to low resolution by comparing the spatial resolution and filter application at the shooting time.

A DJI Mavic2 Pro model drone was used to record the videos, and automatic navigation was performed using Pix4Dcapture with a shooting area of 0.67 km^2 (70 × 95 m^2), flight speed of 10 m/s longitudinal, lateral overlap of 80%, and shooting angle of 90°.

3.2   Reference point surveying and orthographic mapping

In preparation for the aerial survey of the test target area, six ground reference points and two inspection points were installed, as shown in Fig. 3, in accordance with the "Public Survey Work Guidelines for Using Unmanned Aerial Vehicles." In addition, 16 reference points traversing the center of the target river were surveyed using GNSS to calculate the parameters of the pixel value of each band through multiple linear regression analysis. The measurement results of 367 test points were obtained to verify the accuracy of the bathymetric estimation formula.

Table 1
Specified study conditions.

| Type	Time	GSD (cm)	CPL filter	Altitude (m)	Number of images
Case1	10:00	1.0	Not used	50	66
Case2	10:00	1.0	Used	50	66
Case3	10:00	2.5	Not used	100	24
Case4	10:00	2.5	Used	100	24
Case5	12:00	1.0	Not used	50	66
Case6	12:00	1.0	Used	50	66
Case7	12:00	2.5	Not used	100	24
Case8	12:00	2.5	Used	100	24
Case9	15:00	1.0	Not used	50	66
Case10	15:00	1.0	Used	50	66
Case11	15:00	2.5	Not used	100	24
Case12	15:00	2.5	Used	100	24
Case13	12:00	5.0	Used	—	—
Case14	12:00	10.0	Used	—	—
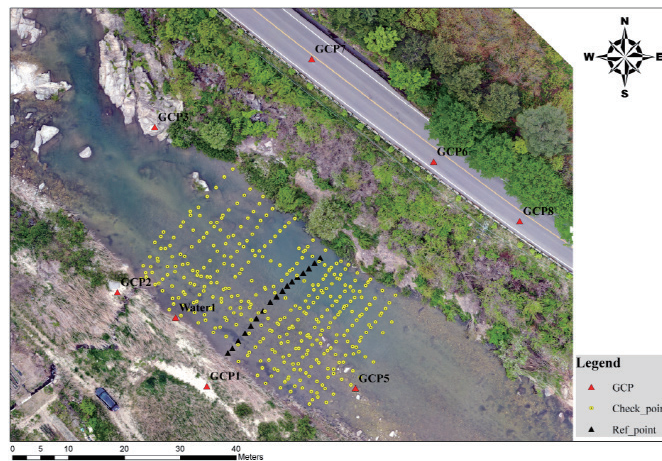
Fig. 3. (Color online) Location of GCP (ground control point) (red), check points (yellow), and reference points (black).

3.3   Symmetry estimation using multiple linear regression analysis

The water depth was estimated by processing the images with multiple linear regression analysis. First, the QGIS software was used to extract the pixel values of the RGB bands of the 16 reference points from the images taken with the drone, and the pixel values of the gray bands were calculated using Eq. (5). Using the extracted pixel value and the actual depth of the reference point, we derived the parameters and constant value for each band for each respective case with the aid of multiple linear regression analysis. The results are listed in Table 2.

Using the values of the four indices and the constant for each band in Table 2, the values for Case 6 can be derived using the depth estimation formula Eq. (7).

Table 2
Calculated values of the indices and constant of each case.

Type	Parameters and constant of each case				
	x_1	x_2	x_3	x_4	C
Case1	0.0073	0.0956	0.0568	−0.0876	−0.5596
Case2	0.1236	0.2020	0.1872	−0.2947	0.2458
Case3	0.0308	0.1122	0.0794	−0.1275	0.2015
Case4	−0.0200	0.0444	0.0349	−0.0310	−0.2130
Case5	0.2369	0.3394	0.2919	−0.4997	0.1801
Case6	−0.0630	−0.0110	−0.0261	0.0582	0.7112
Case7	−0.0840	−0.0452	−0.0354	0.0967	0.6677
Case8	−0.0942	−0.0400	−0.0443	0.1056	0.4625
Case9	0.0353	0.1068	0.0798	-0.1237	−0.1874
Case10	0.1086	0.1842	0.1624	−0.2650	1.1800
Case11	−0.1392	−0.0764	−0.1131	0.1919	−0.0377
Case12	0.1170	0.2492	0.1374	−0.2860	−0.9110
Case13	−0.0544	0.0005	−0.0137	0.0408	0.5018
Case14	−0.1107	−0.0550	−0.0687	0.1362	0.5119

$$y = -0.0630 \cdot R_{band} - 0.0110 \cdot G_{band} - 0.0261 \cdot B_{band} + 0.0582 \cdot Gray_{band} + 0.7112 \qquad (7)$$

Here, y is the water depth and x is the parameter for the DN of each band.

Table 3 presents the measured depth for each of the 16 reference points and the estimated depth value for each of these points for each case specified in Table 1 and calculated using Eq. (7).

3.4 Accuracy analysis depending on drone shooting conditions

The dependence of the accuracy on the conditions under which the drone captured the images was analyzed by comparing the depth of each reference point and the pixel value extracted from the drone image with the actual and estimated depths values at 367 test points employing the parameters calculated using multiple linear regression analysis. The permissible margin of error for bathymetry is stipulated in the "General Survey Work Regulations" for the bathymetry of river clearance works [Article 50 (4)], and the margin of error is ±0.2 m or less if the water depth is no greater than 5 m. Because the water depth in the target area of this study is at most 2 m, we analyzed whether the specified error range was satisfied.

The results of the accuracy analysis by comparing the values of the actual and estimated depths at each of the inspection points for each case are presented in Table 4. Cases 13 and 14 were excluded from the overall accuracy comparison as they were cases in which the drone image of Case 6 was converted to low resolution and compared with regard to spatial resolution. The standard deviation for the photograph captured at 12:00 with low shadows at a spatial resolution of 1 cm and after removing reflected light (Case 6) is ±0.129.

The dependence of the accuracy on the presence or absence of light reflected from the surface of the water was determined by comparing the mean ±0.162 of the standard deviations

Table 3
Comparison of field-surveyed water depth and estimated water depth for Cases 1–14.

No.	Depth	Estimated depth (m)													
		Case1	Case2	Case3	Case4	Case5	Case6	Case7	Case8	Case9	Case10	Case11	Case12	Case13	Case14
Ref.01	0.230	0.318	0.291	0.212	0.267	0.323	0.205	0.251	0.239	0.247	0.215	0.226	0.215	0.183	0.200
Ref.02	0.286	0.409	0.291	0.330	0.279	0.407	0.326	0.390	0.299	0.237	0.321	0.339	0.429	0.354	0.343
Ref.03	0.624	0.536	0.854	0.674	0.894	0.756	0.649	0.716	0.589	0.643	0.530	0.630	0.834	0.660	0.678
Ref.04	0.654	0.540	0.745	0.733	0.735	0.667	0.738	0.508	0.649	0.668	0.755	0.634	0.749	0.682	0.648
Ref.05	0.589	0.507	0.583	0.692	0.635	0.461	0.582	0.730	0.671	0.576	0.554	0.528	0.545	0.596	0.587
Ref.06	0.616	0.603	0.527	0.534	0.532	0.532	0.680	0.523	0.518	0.591	0.573	0.681	0.387	0.639	0.654
Ref.07	0.774	0.777	0.712	0.626	0.765	0.647	0.681	0.651	0.749	0.871	0.824	0.752	0.839	0.726	0.691
Ref.08	0.795	0.895	0.725	0.797	0.788	0.749	0.750	0.805	0.922	0.845	0.901	0.727	0.979	0.724	0.769
Ref.09	1.033	1.181	1.208	1.059	1.153	1.259	1.019	1.145	1.247	1.112	1.097	1.121	1.079	1.081	1.112
Ref.10	1.300	1.191	0.995	1.232	0.887	1.254	1.290	1.240	1.292	1.241	1.245	1.337	1.159	1.282	1.218
Ref.11	1.472	1.457	1.399	1.511	1.432	1.532	1.392	1.477	1.344	1.359	1.412	1.415	1.130	1.401	1.365
Ref.12	1.515	1.478	1.488	1.443	1.555	1.401	1.389	1.460	1.493	1.614	1.470	1.454	1.381	1.380	1.439
Ref.13	1.509	1.372	1.500	1.489	1.473	1.323	1.523	1.444	1.448	1.482	1.313	1.547	1.453	1.563	1.553
Ref.14	1.483	1.602	1.500	1.509	1.488	1.511	1.597	1.526	1.465	1.508	1.557	1.417	1.521	1.485	1.479
Ref.15	1.561	1.444	1.498	1.564	1.509	1.529	1.475	1.591	1.633	1.558	1.600	1.492	1.498	1.520	1.533
Ref.16	1.304	1.432	1.430	1.340	1.352	1.394	1.447	1.288	1.187	1.192	1.377	1.445	1.547	1.467	1.478
Avg.	0.984	0.984	0.984	0.984	0.984	0.984	0.984	0.984	0.984	0.984	0.984	0.984	0.984	0.984	0.984
Max.	1.561	1.602	1.500	1.564	1.555	1.532	1.597	1.591	1.633	1.614	1.600	1.547	1.547	1.563	1.553
Min	0.230	0.318	0.291	0.212	0.267	0.323	0.205	0.251	0.239	0.237	0.215	0.226	0.215	0.183	0.200

Table 4
Results of accuracy analysis for each case.

Type	Average	Minimum	Maximum	Standard deviation	Number of error points exceeding the tolerance	Error rate (%)
Case1	−0.055	−0.457	1.053	0.162	76	20.7
Case2	0.088	−0.786	0.555	0.176	108	29.4
Case3	−0.016	−0.505	0.408	0.143	60	16.3
Case4	−0.034	−0.478	0.493	0.146	60	16.3
Case5	0.084	−0.370	1.015	0.204	108	29.4
Case6	−0.021	−0.473	0.286	0.129	44	12.0
Case7	−0.011	−0.624	0.438	0.166	72	19.6
Case8	−0.043	−0.737	0.479	0.155	66	18.0
Case9	−0.092	−0.440	0.379	0.148	97	26.4
Case10	−0.036	−0.631	0.579	0.180	92	25.1
Case11	−0.050	−0.522	0.411	0.148	71	19.3
Case12	−0.134	−0.612	0.629	0.203	158	43.1
Case13	0.006	−0.492	0.391	0.134	47	12.8
Case14	−0.017	−0.370	0.249	0.104	21	5.7

calculated for images captured without the polarizing filter (Cases 1, 3, 5, 7, 9, and 11), with the mean ±0.165 of those acquired with the polarizing filter (Cases 2, 4, 6, 8, 10, and 12), the difference is 0.003 m. To analyze the effect of shadows on the accuracy, the average of the standard deviations at each shooting time was calculated for comparison. The mean of the standard deviations for images captured at 10:00 (Cases 1, 2, 3, and 4) is ±0.157, that for images captured at 12:00 (Cases 5, 6, 7, and 8) is ±0.163, and that for images captured at 15:00 (Cases 5,

6, 7, and 8) is ±0.170. However, an examination of individual cases revealed that the images taken at 12:00 are the most accurate. Analysis of the results of the case with the highest accuracy (Case 6) and the results obtained for the cases that were converted to low resolution using Case 6 (Cases 13 and 14), revealed that the accuracy with respect to the spatial resolution decreases slightly with conversion to the lower resolution. Nonetheless, because the average pixel value is applied, the higher accuracy is attributed to the conversion of the pixel value to lower resolution.

With respect to the error rate, the estimated depth in Case 6 was analyzed using inspection points, and it was found that there were 44 inspection points outside the error tolerance of ±0.2 m, accounting for about 12.0% of the total. The results indicate that nearly 88.0% of the total values were within the specified error tolerance, and in Case 14, about 94.3% of the total values were within the error tolerance with 21 inspection points.

The results of the analysis of the measured depth vs the estimated depth are presented in the form of scatter plots in Fig. 4. These results were obtained for images taken at 12:00 and a spatial resolution of 1 cm (Case 6) with the use of a polarizing filter. The value of R^2 is 0.980, and when the spatial resolution of images taken at 12:00 is converted to 10 cm (Case 14), the value of R^2 is 0.987, indicating that the estimated value is closer to the actual value.

3.5 Results of cause-of-error analysis and discussion

The cause of the error in the estimation was investigated on the basis of the case in which the images were photographed at 12:00 with a spatial resolution of 1 cm (Case 6) and a polarizing filter was used. As a result, in the case of region A in Fig. 5, an error occurred because the pixel values differed from those in the original topography due to the shadow in the river bed. In the case of region B, referring to a reported method used to analyze drone images acquired via optical remote sensing,[1] the results showed that the tolerance range was within 1.6 m after applying the polarization filter (the estimated depth was 1.4 m), indicating that the actual depth in the b-2 area is 1.663 m. In the case of the b-1 area, the actual depth is 1.142 m, but the pixel values were found to be distorted owing to shadows between the rocks on the river bed, thereby giving rise to a large error. In the case of the b-3 area, the actual depth is 1.435 m, but the water surface was found to be disturbed by wind. This distorted the pixel value, resulting in a large error. To summarize, the results of this study showed that it is difficult to apply the proposed method to shallow rivers with a maximum depth of approximately 1.6 m, particularly when the flow rate is high, windy conditions exist, the water is deep with high turbidity, and algae and aquatic vegetation are present in abundance.

A comparison of the results obtained using the numerical topographic model based on optical remote sensing with those obtained using the conventional method employing survey data indicates that the calculated topography is higher than that of the actual terrain when only the image taken by the drone is used [Figs. 6(d) and 6(e)]. The elevation determined by the direct survey method corresponds to the actual lower elevation, but, because the obtained value is small, it is not possible to show a detailed river topography, as shown in Figs. 6(b) and 6(e). However, the optical remote sensing technique can determine the exact downstream elevation value, and a detailed downstream topography is obtained, as shown in Figs. 6(c) and 6(f).
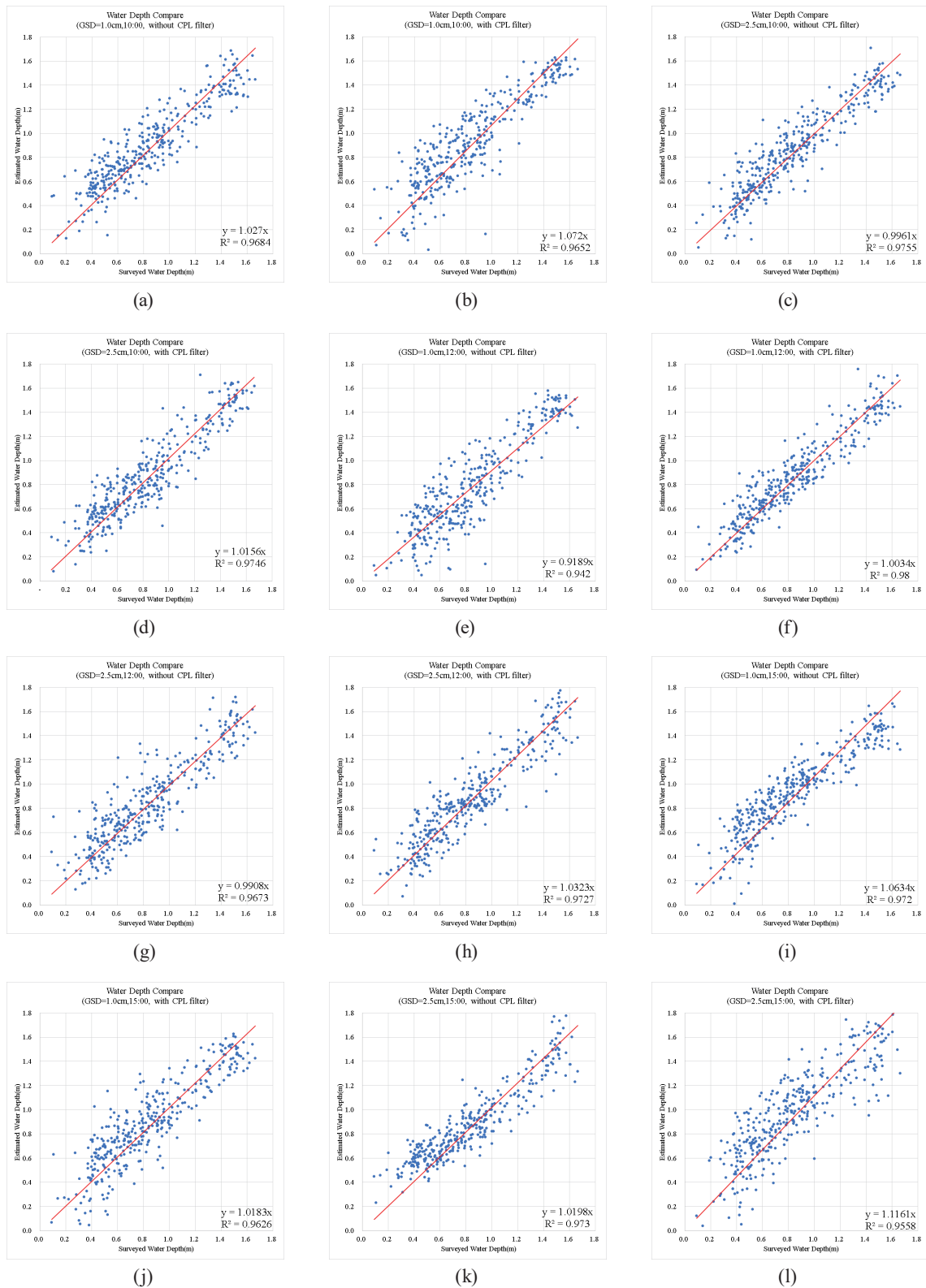
Fig. 4. (Color online) Depth determined in the field survey and estimated depth: (a) Case 1, (b) Case 2, (c) Case 3, (d) Case 4, (e) Case 5, (f) Case 6, (g) Case 7, (h) Case 8, (i) Case 9, (j) Case 10, (k) Case 11, (l) Case 12, (m), Case 13, and (n) Case 14.
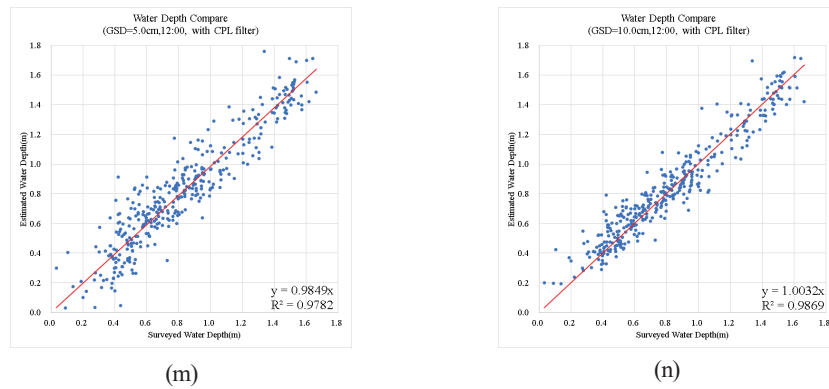
(m)

(n)

Fig. 4.   (Continued) (Color online) Depth determined in the field survey and estimated depth: (a) Case 1, (b) Case 2, (c) Case 3, (d) Case 4, (e) Case 5, (f) Case 6, (g) Case 7, (h) Case 8, (i) Case 9, (j) Case 10, (k) Case 11, (l) Case 12, (m), Case 13, and (n) Case 14.
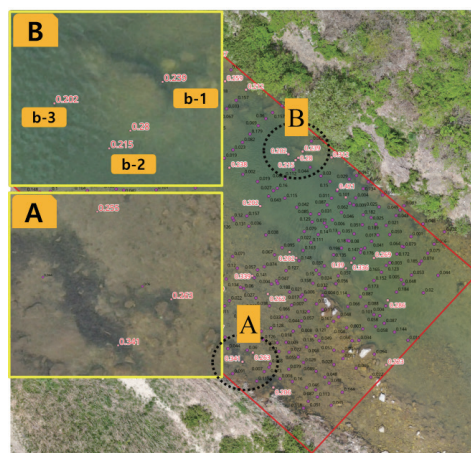

Fig. 5.   (Color online) Locations of points for which the accuracy was the lowest.

(a)   (b)   (c)

(d)   (e)   (f)
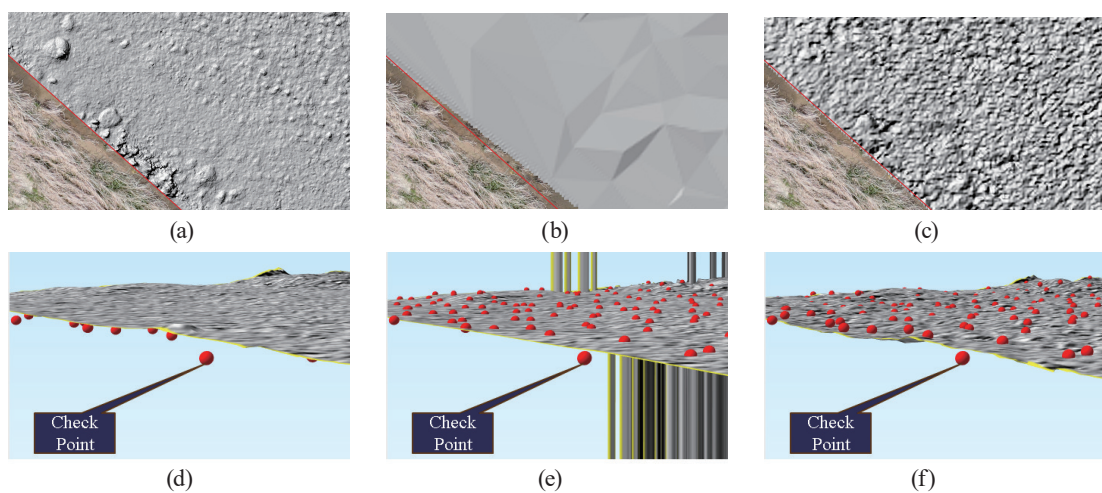
Fig. 6.   (Color online) Digital elevation model (DEM) of study area. Relief shaded terrain (Hillshade) views of the (a) image captured by the drone, (c) surveyed data, and (e) estimated data. 3D renderings of the (b) image taken by the drone, (d) surveyed data, and (f) estimated data.

4.　　Conclusions

In this paper, the results obtained by our method of estimating the depth of shallow rivers using an optical remote sensing technique to capture high-resolution images with a drone are presented.

First, calculation of the pixel value for each band of the image and calculation and estimation of the directly measured depth value by multiple linear regression analysis enabled the depth of a shallow river to be estimated more efficiently than by the existing direct survey method.

Second, when the images that were captured by the drone with polarizing filters to remove the light reflected from the surface and when high-resolution images were taken at noon without shadows, the accuracy of the depth at about 88% of the positions in a shallow river (of which the depth does not exceed 1.6 m), was within the allowable range of bathymetry, and when converted to low resolution, about 94% of the results were within the allowable range.

Third, the accuracy of depth estimation using optical remote sensing techniques was found to be low for greater depths, and errors may occur owing to the distortion of pixel values by water plants or shadows.

In the future, research on depth estimation under more diverse environmental conditions, such as an assessment of the effect of water turbidity, and additional depth estimation methods, such as the use of artificial intelligence to eliminate errors introduced by shadows, will be required.

Acknowledgments

References

1　B. G. Choi and Y. W. Na: J. Korean Soc. Surv. Geod. Photogramm. Cartogr. **40** (2022) 635 (in Korean). https://doi.org/10.7848/ksgpc.2022.40.6.635

2　J. S. Ehses and J. J. Rooney: NOAA Technical Memorandum NMFS-PIFSC **46** (2015) 24. https://doi.org/10.7289/V5668B40

3　J. B. Lee, H. J. Kim., J. H. Kim, and G. J. Wie: J. Korean Soc. Surv. Geod. Photogramm. Cartogr. **39** (2021) 235 (in Korean). https://doi.org/10.7848/ksgpc.2021.39.4.235

4　C. Y. Oh, K. M. Ahn, J. S. Park, and S. W. Park: J. Korean Soc. Coastal. Ocean. Eng. **29** (2017) 162 (in Korean). https://doi.org/10.9765/KSCOE.2017.29.3.162

5　R. A. Holman, K. L. Brodie, and N. J. Spore: IEEE Trans. Geosci. Remote Sens. **55** (2017) 2017. https://doi.org/10.1109/TGRS.2016.2635120

6　J. H. Yi, K. H. Ryu, C. J. Shin, W. D. Baek, and W. M. Jung: J. Korean Soc. Hazard. Mitigation **16** (2016) 351 (in Korean).　https://doi.org/10.9798/KOSHAM.2016.16.5.351

7　H. J. Yeo, S. P. Choi, and Y. Yeu: J. Korean Soc. Geospatial Inf. Sci. **24** (2016) 3 (in Korean). https://doi.org/10.7319/kogsis.2016.24.1.003

8　W. D. Philpot: J. Opt. Soc. Am. A **28** (1989) 1569. https://doi.org/10.1364/AO.28.001569

9　D. R. Lyzenga, N. P. Malinas, and F. J. Tanis: IEEE Trans. Geosci. Remote Sens. **44** (2006) 2251. https://doi.org/10.1109/TGRS.2006.872909

About the Authors

Byoung Gil Choi received his B.S., M.S., and Ph.D. degrees from Hanyang University, Korea, in 1984, 1986, and 1992, respectively. Since 1992, he has been a professor at Incheon National University. His research interests are in drones, GIS, and remote sensing. (bgchoi@inu.ac.kr)

Yong Hee Kwon received his B.S. degree from Hankyong University, Korea, in 1998 and his M.S. and Ph.D. degrees from Incheon National University, Korea, in 2010 and 2023, respectively. Since 1986, he has been an engineer at several civil engineering companies. His research interests are in drones, GIS, and remote sensing. (kwonyhee@nate.com)

Jun Hee Lee received his B.S. degree from Seoul National University of Science & Technology, Korea, in 2010, Since 1995, he has been an engineer at several civil engineering companies. His research interests are in drones, GIS, and remote sensing. (hiboss@nate.com)

Young Woo Na received his B.S., M.S., and Ph.D. degrees from Incheon National University, Korea, in 2001, 2003, and 2009, respectively. From 2009 to 2021, he was a researcher and assistant professor at Incheon National University, Korea. Since 2021, he has been an assistant professor at Semyung University. His research interests are in drones, GIS, and remote sensing. (survey21@semyung.ac.kr)